

REPORT DOCUMENTATION PAGE			Form Approved OMB No. 0704-0188	
Public reporting burden for this collection of information is estimated to average 1 hour per response, including the time for reviewing instructions, searching existing data sources, gathering and maintaining the data needed, and completing and reviewing the collection of information. Send comments regarding this burden estimate or any other aspect of this collection of information, including suggestions for reducing this burden, to Washington Headquarters Services, Directorate for Information Operations and Reports, 1215 Jefferson Davis Highway, Suite 1204, Arlington, VA 22202-4302, and to the Office of Management and Budget, Paperwork Reduction Project (0704-0188), Washington, DC 20503.				
1. AGENCY USE ONLY (Leave blank)		2. REPORT DATE NOVEMBER 2003		3. REPORT TYPE AND DATES COVERED USARIEM TECHNICAL REPORT
4. TITLE AND SUBTITLE THE ROLE OF SOLAR AND UV RADIATION IN ENVIRONMENTAL STRESS ASSESSMENT			5. FUNDING NUMBERS	
6. AUTHOR(S) DANIEL S. MORAN, KENT B. PANDOLF, ANTONIOS VITALIS, YUVAL HELED, RICHARD PARKER, AND RICHARD R. GONZALEZ				
7. PERFORMING ORGANIZATION NAME(S) AND ADDRESS(ES) U.S. Army Research Institute of Environmental Medicine Biophysics & Biomedical Modeling Division Kansas Street Natick, MA 01760-50076			8. PERFORMING ORGANIZATION REPORT NUMBER T04-01	
9. SPONSORING / MONITORING AGENCY NAME(S) AND ADDRESS(ES) U.S. Army Medical Research and Materiel Command Fort Detrick, MD 21702-5007			10. SPONSORING / MONITORING AGENCY REPORT NUMBER	
11. SUPPLEMENTARY NOTES				
12a. DISTRIBUTION / AVAILABILITY STATEMENT Approved for public release; distribution unlimited			12b. DISTRIBUTION CODE	
13. ABSTRACT (Maximum 200 words) <p>Meteorological variables, including ambient temperature, wet bulb temperature, black globe temperature, wind velocity, relative humidity, global radiation (GR), and ultraviolet (UV) radiation, were measured in Israel and New Zealand. The purpose of this study was to evaluate the role of solar and UV radiation components in environmental stress assessment and to test the contribution of UV radiation in the environmental stress index (ESI). The weight for each parameter from which ESI and WBGT were constructed, and the contribution of the UV radiation to the thermal load were evaluated in an attempt to include the UV radiation in ESI. Data analysis revealed that UV radiation did not contribute to ESI and that GR in ESI was sufficient for thermal load assessment. In conclusion, ESI should include GR spectrum (280-2800nm) rather than UV radiation spectrum (280-400 nm). However, because of the health hazards of UV radiation, an independent index parallel to the ESI should be considered and used for safety measures and as guidelines for protection from UV radiation. The UV index has greater potential for acceptance by laymen if GR is incorporated in its derivation, which is a more commonly measured and used variable than UV radiation.</p>				
14. SUBJECT TERMS Keywords: heat, index, global radiation, thermal load, ozone layer			15. NUMBER OF PAGES 40	
			16. PRICE CODE	
17. SECURITY CLASSIFICATION OF REPORT U	18. SECURITY CLASSIFICATION OF THIS PAGE U	19. SECURITY CLASSIFICATION OF ABSTRACT U	20. LIMITATION OF ABSTRACT U	

USARIEM TECHNICAL REPORT T04-01

**THE ROLE OF SOLAR AND UV RADIATION IN
ENVIRONMENTAL STRESS ASSESSMENT**

**Daniel S. Moran
Kent B. Pandolf
Antonios Vitalis
Yuval Heled
Richard Parker
Richard R. Gonzalez**

Biophysics and Biomedical Modeling Division

November 2003

**U.S. Army Research Institute of Environmental Research
Natick, MA 01760-5007**

TABLE OF CONTENTS

<u>SECTION</u>	<u>PAGE</u>
List of Figures.....	iv
List of Tables.....	vi
Acknowledgments	vii
List of Abbreviations	viii
Executive Summary	1
Introduction	2
Military Relevance	4
Methods	5
Measurements.....	5
Calculations	6
Statistical Analysis.....	6
Results	6
Study I - Israel	6
UV Radiation	11
Study II – New Zealand	17
Validation of ESI	24
Discussion	27
Conclusions.....	28
References.....	30
Appendix A.....	32

LIST OF FIGURES

<u>FIGURE</u>		<u>PAGE</u>
1	Comparison of a newly developed model (I) based on ambient temperature (T_a), with the residuals scattergram (top) and WBGT index showing correlation (bottom). Database for this figure was collected from three stations in Israel	9
2	Comparison of a newly developed model (II) based on T_a and relative humidity (RH), with the WBGT index showing correlation (bottom) and residuals scattergram (top). Database for this figure was collected from three stations in Israel	10
3	Comparison of a newly developed model (III) based on T_a , RH and solar radiation (SR) with WBGT index showing residuals scattergram (top) and correlation (bottom). Database for this figure was collected from three stations in Israel.	11
4	Comparison of a newly developed model (IV) based on T_a , RH, SR and wind velocity (V_a), with the WBGT index showing correlation (bottom) and residuals scattergram (top). Database for this figure was collected from three stations in Israel	13
5	Comparison of a newly developed model (V) based on T_a , RH, SR, V_a and ultraviolet radiation (UV), with the WBGT index showing correlation (bottom) and residuals scattergram (top). Database for this figure was collected from three stations in Israel	14
6	Comparison of a newly developed model (VI) based on T_a , RH, SR, V_a and $UV > 0.4 \text{ W} \cdot \text{m}^{-2}$, with the WBGT index showing correlation (bottom) and residuals scattergram (top). Database for this figure was collected from three stations in Israel	15
7	Comparison of a newly developed model (VII) based on T_a , RH, V_a and UV, with the WBGT index showing correlation (bottom) and residuals scattergram (top). Database for this figure was collected from three stations in Israel	16

FIGUREPAGE

8	Validation of the newly developed model (I) based on T_a , with the WBGT index showing correlation (bottom) and residuals scattergram (top). Database for this figure was collected from two stations in New Zealand	19
9	Validation of the newly developed model (II) based on T_a and RH, with the WBGT index showing correlation (bottom) and residuals scattergram (top). Database for this figure was collected from two stations in New Zealand	20
10	Validation of the newly developed model (III) based on T_a , RH and SR, with the WBGT index showing correlation (bottom) and residuals scattergram (top). Database for this figure was collected from two stations in New Zealand	21
11	Validation of the newly developed model (IV) based on T_a , RH, SR and V_a , with the WBGT index showing correlation (bottom) and residuals scattergram (top). Database for this figure was collected from two stations in New Zealand	22
12	Validation of the newly developed model (VI) based on T_a , RH, SR, V_a and $UV > 0.4 \text{ W}\cdot\text{m}^{-2}$, with the WBGT index showing correlation (bottom) and residuals scattergram (top). Database for this figure was collected from one station in New Zealand	23
13	Comparison of the ESI, with the WBGT index showing correlation (bottom) and residuals scattergram (top). Database for this figure was collected from three stations in Israel	25
14	Comparison of the ESI, with the WBGT index showing correlation (bottom) and residuals scattergram (top). Database for this figure was collected from two stations in New Zealand	26

LIST OF TABLES

<u>TABLE</u>		<u>PAGE</u>
1	Mean (\pm SD) and range of environmental measurements collected in New in Israel. Data were collected from three different locations every 10 min over 24 hours for 120 days during June-September.	7
2	Mean (\pm SD) and range of environmental measurements collected in New Zealand. Data were collected from 2 different locations every 10 min over 24 hours for 60 days during February-March	17
3	The correlation coefficient (R^2) between the WBGT index and the different predicted models, developed from the Israeli database and validated for the New Zealand database.	18

ACKNOWLEDGMENTS

This work was conducted in Israel and New Zealand as part of a cooperative effort between the US Army Research Institute of Environmental Medicine (USARIEM)/Israel Defense Force Biophysics and Biomedical Modeling effort, and with the Center for Human Factors and Ergonomics (COHFE) and Massey University. Dr. Arie Laor and Ms. Liron Shalit's contributions in the statistical analysis and evaluation of the different environmental stress indices are appreciated. The authors are also extremely thankful for the cooperation and assistance of Mr. Jacob Mishaeli of the Israeli Meteorological Service.

LIST OF ABBREVIATIONS AND ACRONYMS

COHFE – Center for Human Factors and Ergonomics

ESI – environmental stress index

GR – global radiation ($\text{W}\cdot\text{m}^{-2}$)

IMS – Israeli Meteorological Service

NIWA – National Institute of Water and Atmospheric Research

RH – relative humidity (%)

SR – solar radiation ($\text{W}\cdot\text{m}^{-2}$)

T_a – ambient temperature ($^{\circ}\text{C}$)

T_g – black globe temperature ($^{\circ}\text{C}$)

T_{sk} – skin temperature ($^{\circ}\text{C}$)

T_w – wet bulb temperature ($^{\circ}\text{C}$)

UV – ultraviolet

UVA – electromagnetic radiation of wavelengths in the 320-400 nm range

UVB – electromagnetic radiation of wavelengths in the 280-320 nm range

UVC – electromagnetic radiation of wavelengths in the 220-290 nm range

V_a – wind velocity ($\text{W}\cdot\text{sec}^{-1}$)

WBGT – wet bulb globe temperature ($^{\circ}\text{C}$)

EXECUTIVE SUMMARY

The purpose of this study was to evaluate the role of solar and UV radiation components in environmental stress assessment and to test the contribution of the UV radiation variable in a modified environmental stress index (ESI).

Meteorological variables, including ambient temperature (T_a), wet bulb temperature (T_w), black globe temperature (T_g), wind velocity (V_a), relative humidity (RH), global radiation (GR), and ultraviolet (UV) radiation, were measured during the summer (June-September) at three locations in Israel, and during the summer (February-March) at two locations in New Zealand. These five databases were used to calculate the wet bulb globe temperature (WBGT) and the environmental stress index (ESI).

Accordingly, analysis of the weight for each parameter from which ESI and WBGT were constructed was evaluated from the three databases collected in Israel, and validated for the two databases collected in New Zealand. In addition, the weight and the contribution of the UV radiation to the thermal load were evaluated in an attempt to include it as a variable in a new modified ESI. These data were collected every 10 min over 24 hr and contained over 51,000 measurements for each variable in Israel, and over 18,000 measurements for each variable in New Zealand.

For the development of the modified ESI we constructed a series of models for WBGT and ESI as dependent variables, and for T_a , T_w , RH, GR, V_a and UV radiation as independent variables. Data and statistical analysis revealed that the UV radiation did not contribute to the environmental stress assessment and that the GR component in the ESI was sufficient for heat load assessment. Furthermore, mathematically, the UV radiation was found to be a negative term in the modified ESI. This is probably due to the fact that the UV component was already included in the GR spectrum.

In conclusion, the ESI should include the GR spectrum (280-2800nm) rather than UV radiation spectrum (280-400 nm) component. However, because of the health hazards of UV radiation, an independent index parallel to the ESI should be considered and used for safety measures and as guidelines for protection from UV radiation. The UV index has greater potential for acceptance by laymen if GR is incorporated in its derivation, which is a more commonly measured and used variable than UV radiation.

INTRODUCTION

When considering the heat stress affecting athletes or soldiers in training, the specific contribution of solar radiation (SR) is often overlooked or does not receive the appropriate/necessary attention. This is especially true regarding the long-term consequences of exposure to SR. In fact, the effect of SR is not measured directly in the current, most popular environmental index, the wet bulb globe temperature (WBGT) (24), which is used to measure heat stress and is constructed from ambient temperature (T_a), wet bulb temperature (T_w), and black globe temperature (T_g).

In 2001, a new environmental stress index (ESI) was suggested (14). This new index is constructed from the measurement of T_a , relative humidity (RH) and SR. However, the SR component does not differentiate between types of radiations, such as ultraviolet (UV), which can be dangerous and is considered a potential health hazard.

To understand the risk incurred by solar SR, it is necessary to understand how SR injures living tissue. In fact, only light with a wavelength in the UV range of the spectrum (220-400 nm) causes damage. Most UV light is absorbed by the ozone layer of the stratosphere or reflected back into space, so only a small amount reaches the surface of the earth (7). UV light is also easily scattered by air molecules and therefore even reaches shaded areas apparently protected from direct sunrays. Typical window glass transmits about 3%-4% of UV light, thereby not providing complete protection (13).

Since the 1970s, scientists have realized that Chlorofluorocarbons (CFCs) in commercial aerosols deplete the ozone layer by an average of 3% (23). CFCs have a long half-life and contain high concentrations of chlorine, which reacts catalytically with ozone. At high latitudes, the ozone depletion is greater by up to 8%. Thus, the corresponding effect of the increased penetration of UV light into the atmosphere differs depending mainly on the geographic location (10).

Beginning in the 1980s, the status of the ozone layer and the corresponding changes in the transmission of UV radiation have been monitored by the World Meteorological Organization (WMO), as well as by many regional and national environmental agencies. The measurements and surveys conducted by these organizations determined that a large *ozone hole* had developed over Antarctica, and a smaller one over the Arctic Circle. Apparently, the cold atmosphere in the Polar Regions amplifies the destructive ability of CFCs. Thus, countries close to the regions of the greatest ozone depletion, such as Australia and New Zealand, incur a *calculated* 15% greater exposure to UV radiation than countries in the northern hemisphere. However, the *measured* difference between the hemispheres is much larger, with 50%-80% more UV radiation in New Zealand, at 45S latitude, than in the latitudes of northern Europe and North

America at 48N latitude (19). This can be related to the relative thinness of the ozone layer in the southern hemisphere, and the fact that the southern hemisphere is closer to the sun during the summer months. The amount of UV light reaching the ground is also affected by the height of the sun and the cloudiness of the sky. When the sun is higher in the sky at midday, its rays pass directly through the atmosphere before striking the ground. Conversely, when the sun is lower in the sky, its rays must pass obliquely through the atmosphere before reaching the ground, thus passing through a thicker ozone column. Thus, most of the daily cumulative UV energy is accrued during the two-hour period centered on the solar noon. Clouds reflect UV light back into the atmosphere, but must be thick and extensive to afford appreciable protection from UV radiation.

In dry climates like the Middle East, where there are infrequent periods of thick cloud cover even in the winter, and where there is a relatively high frequency of clear, sunny days, the exposure to UV radiation is significant. People with outdoor occupations and hobbies, children and athletes, and soldiers in training or performing tasks in the open air are at great risk from UV radiation.

To quantify this risk, the WMO has recommended that countries at risk adopt and publicize a UV Index (12). This index should correspond to the "burn time" of sensitive skin during exposure to SR at midday and sun burning UV radiation (in units of $\text{W}\cdot\text{m}^{-2}$) multiplied by a factor of 40 (12). However, even this index does not take into account the long-term implications of prolonged exposure to UV radiation. Aside from the acute effects of sun exposure related to heat stress and sunburn, SR can cause severe injury to the skin and related structures. Some of these injuries present clinically only after many years, and they can be fatal.

In fact, chronic exposure to SR has been linked to increased risk of the three most common skin cancers; Basal Cell Carcinoma (BCC), Squamous Cell Carcinoma, and Malignant Melanoma (2). Ultraviolet radiation from sun exposure also causes sunburn, pigmentation, epithelial hyperplasia, local immunosuppression, DNA damage, and premature actinic aging of the skin and associated structures (1). The incidence rate of the skin cancers and the above-mentioned effects is higher in fair-skinned, sun-sensitive persons, and occurs mostly on the exposed parts of the body to the sun. Moreover, exposure to high levels of sunlight early in childhood is a strong determinant of skin cancer risk (22). Even relatively short periods of exposure, such as during sports and holidays, are associated with increased risk of BCC (18).

The energy of SR is inversely proportional to the wavelength. The wavelength at which this energy begins to damage biological tissues is in the UV spectrum, just below visible light (5). UVB (280-320 nm) and, to some extent UVA (320-400 nm) are the radiation wavelengths associated with actinic damage. UVC (220-290 nm) is even more potent, but is completely absorbed by ozone and other molecules in the stratosphere and does not reach the ground.

The UV radiation alters the quantity and structure of the extracellular matrix by suppressing messenger ribonucleic acid (mRNA) transcription of matrix proteins, possibly via the stimulation of cytokines such as IL-1-alpha (21). The outcome of the extracellular matrix damage is actinic elastosis/lysis, resulting in skin atrophy and roughening. Superficial subdermal structures, such as blood vessels, may also be affected by SR to produce granulomatous changes such as temporal arteritis (16). UV radiation also leads to the development of premature cataracts by injuring cell membrane ionic pumps and critical enzymes, as well as protein synthesis (6). There is also evidence that UV radiation may activate viruses and impair immunity. Activation of HIV infection in the summer was reported in patients with AIDS (20). UV radiation inhibits the antigen presenting function of macrophages, and the apoptotic and cell-lytic functions of natural killer cells (9). UV radiation also undermines the p53 tumor suppressor gene (4). All these factors combined lead to the disastrous result that every *third* person in New Zealand contracts skin cancer (3).

The purpose of this study was to evaluate the role of the UV radiation component in the environmental stress assessment and to test its contribution to the ESI. An attempt to develop and construct an environmental stress index that includes the UV radiation component would be executed. This newly developed index might be used as a guideline for different outdoor activities for civilians and military in order to prevent health hazards related to environmental stress, SR and UV radiation.

MILITARY RELEVANCE

The practical implication of this information on the military is that the exposure to SR, especially the UV component, must be taken into account when calculating the environmental stress imposed on soldiers during outdoor exposure. The effect of SR is not precisely introduced in the current heat stress indices, and pertains to both immediate and chronic consequences for soldiers serving outdoors. Furthermore, those at risk are not only soldiers in training, but also all persons engaged in outdoor activity of any kind, such as sentries, gardeners, and construction and maintenance workers. This phenomenon differs around the globe, depending on the geographical zone. Therefore, an environmental stress index that includes the UV radiation component should be implemented, and a corresponding activity and protection protocol developed to protect both military and civilian populations from the hazards of SR, especially for those who are nearer to Antarctica and the Arctic Circle.

METHODS

Meteorological parameters including V_a , T_g , T_a , SR, RH, and UV radiation were measured in Israel and New Zealand. Data were collected continuously over a period of 4 months (June-September) at three different locations in Israel, and over a period of 2 months (February-March) at two locations in New Zealand. In Israel, data were collected in Sdom, located on the Dead Sea West Shore at latitude 31.09N, longitude 35.15E, Jerusalem; located at latitude 31.93N, longitude 34.59E; and in the Tel Aviv area, located at latitude N31.28, longitude 34.32E. These stations are each different in climate and height from sea level (-400, 800, 30 meters, respectively). In New Zealand, data were collected from two stations located on the South Island: Lauder, located at latitude 45.04S, longitude 169.68E; and Christchurch, located at latitude 43.31S, longitude 172.37E. These five databases were used to calculate WBGT and ESI. Accordingly, analysis of the weight for each parameter from which ESI was constructed was evaluated from the three databases collected in Israel and validated for the two databases collected in New Zealand. In addition, the weight and the contribution of UV radiation to the thermal load was evaluated in an attempt to include it as a parameter in a modified environmental stress index.

MEASUREMENTS

The official Israeli Meteorological Service (IMS) collected weather measurements for the three locations. T_a and T_w were measured with Campbell thermometers (model HMP45C), and relative humidity (RH) was measured with a Rotronic instrument (model MP 100A). These three instruments were placed under a shelter (Stevenson screen). Under open sky, T_g was measured using the Vernon black globe thermometer; SR was measured using the EPLAB radiometer (sensitivity of 285-2800 nm), UV and UVB was measured by pyranometer (Yankee Environmental System, Inc., USA) and the V_a was measured by the Young Instrument (Model 05103). In New Zealand, meteorological data was collected by the National Institute of Water and Atmospheric Research (NIWA) at two locations. T_a and RH were measured using a Vaisala probe (Model HMP45D). T_w was derived from these data. T_g was measured using the Vernon black globe thermometer. V_a was measured using a Vector A101M anemometer. SR was measured at the Christchurch station using a LiCor pyranometer (LI200), and at the Lauder station using an Epply PSP radiometer. The UV measurements were recorded from UVB-1 sensors (Yankee Environmental System, Inc). These instruments are designed to measure erythemally weighted UV irradiances (i.e., the UV relevant for causing sunburn in human skin) falling on a horizontal surface. However, because of a slight mismatch between the instrument function and the desired erythema weighting function, a radiative transfer model was used to convert instrument-weighted UV to erythemally weighted UV. Inputs to the model included ozone and sun angle.

The model was also used to correct imperfections in the instrument angular response. Ideally for irradiance measurements, the angular response should follow a cosine curve, but in reality, there are always small departures. Finally, the model was used to convert by mathematical and physics equations the erythemally weighted irradiances to UVB (280-315 nm) irradiances. All data were averaged in 10-minute intervals.

CALCULATIONS

Heat stress indices were calculated as follows: WBGT was calculated according to Yaglou and Minard's standard index; $WBGT = 0.7T_w + 0.2T_g + 0.1T_a$ (20). The newly developed environmental stress index (ESI) was calculated, as follows (21):

$$ESI = 0.62T_a - 0.007RH + 0.002SR + 0.0043(T_a \cdot RH) - 0.078(0.1 + SR)^{-1}$$

A series of new models were developed from the databases collected in this study and will be presented in the Results section.

STATISTICAL ANALYSIS

The collected measurements were analyzed by multiple regression analysis, using the SAS software. For the development of the new ESI or for ESI correction/modification, we constructed a series of models for WBGT and ESI as dependent variables, and T_a , RH, SR, V_a and UV radiation as independent variables. Optimization of these constants was executed by the ("does not use derivative:") DUD method (17). For all models, we computed the coefficient of determination (R-square of the model) and plotted a series of residual plots versus predicted values for all data and for every meteorological station separately. All statistical contrasts were accepted at the $P < 0.05$ level of significance. Data are presented in this study as means \pm SD. For all computations and statistical analysis, we used SAS 8.0 software, Procedures CORR and GLM.

RESULTS

STUDY I – ISRAEL

These data were collected every 10 min over 24 hr for 120 days during June-September. Therefore, a wide range of weather measurements, over 51,000 for each variable, was covered as depicted in Table 1 (mean \pm SD) and for each of the three stations in appendix A (Sdom, Jerusalem, and the Tel-Aviv area).

Table 1. Mean (\pm SD) and range of environmental measurements collected in Israel. Data were collected from three different locations every 10 min over 24 hours for 120 days during June through September.

	T_a ($^{\circ}\text{C}$)	T_w ($^{\circ}\text{C}$)	RH (%)	T_g ($^{\circ}\text{C}$)	SR ($\text{W}\cdot\text{m}^{-2}$)	UV ($\text{W}\cdot\text{m}^{-2}$)	V_a ($\text{m}\cdot\text{sec}^{-1}$)
Mean \pm SD	28.23 \pm 5.82	20.67 \pm 3.02	55 \pm 22	32.85 \pm 9.88	300 \pm 361	6.98 \pm 9.50	3.70 \pm 1.91
Range	13.90-45.40	9.92-27.90	8-102	10.80-60.00	0-1171	0.0-31.51	0.0-12.60

In order to evaluate the weight of each of the environmental variables for heat load and its contribution to the prediction of heat stress assessment, we constructed a series of step wise prediction models.

First, we predicted WBGT only from T_a as follows: (Model I).

$$\text{WBGT} = 0.83351T_a^{\circ}\text{C}; \quad .\text{I}$$

As depicted in Figure 1, the correlation was moderate ($R^2=0.687$). between Model I, which is based only on T_a , and WBGT. However, the residual scattergram was wide and ranged from -6° to 7°C . Next, we constructed a WBGT prediction model from T_a and RH, as follows:

$$\text{WBGT} = 0.71407T_a + 0.06891\text{RH }^{\circ}\text{C}; \quad .\text{II}$$

This prediction model markedly increased the correlation coefficient between calculated and predicted WBGT to $R^2=0.833$ and narrowed the residuals scattergram to a range from -4° to 4°C . However, it was noted that during low environmental stress, this model overestimated the WBGT values, whereas during the higher environmental stress, it underestimated WBGT values (Figure 2). Thus, the next step was to add the SR component for the WBGT prediction model. The new developed prediction model, including SR, was as follows:

$$\text{WBGT} = 0.66219T_a + 0.07681\text{RH} + 0.00346\text{SR }^{\circ}\text{C}; \quad .\text{III}$$

This prediction model revealed high correlation with calculated WBGT ($R^2=0.924$), but as in Model II, overestimation values were observed at low stress, whereas underestimation was revealed for the high stress values (Figure 3).

Figure 1. Comparison of a newly developed model (I) based on ambient temperature (T_a), with the WBGT index showing correlation (bottom) and residuals scattergram (top). Database for this figure was collected from three stations in Israel.

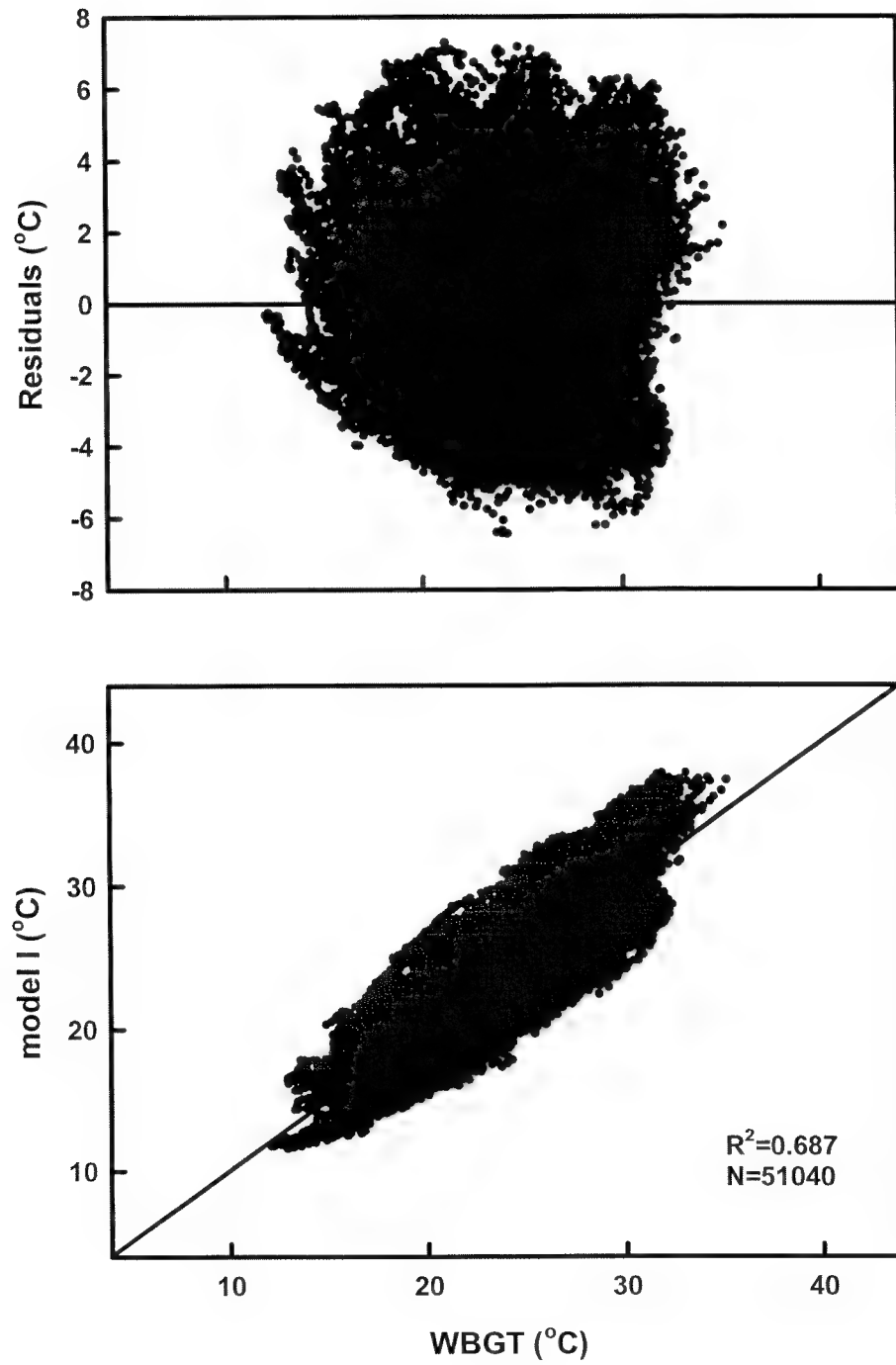


Figure 2. Comparison of a newly developed model (II) based on T_a and relative humidity (RH), with the WBGT index showing correlation (bottom) and residuals scattergram (top). Database for this figure was collected from three stations in Israel.

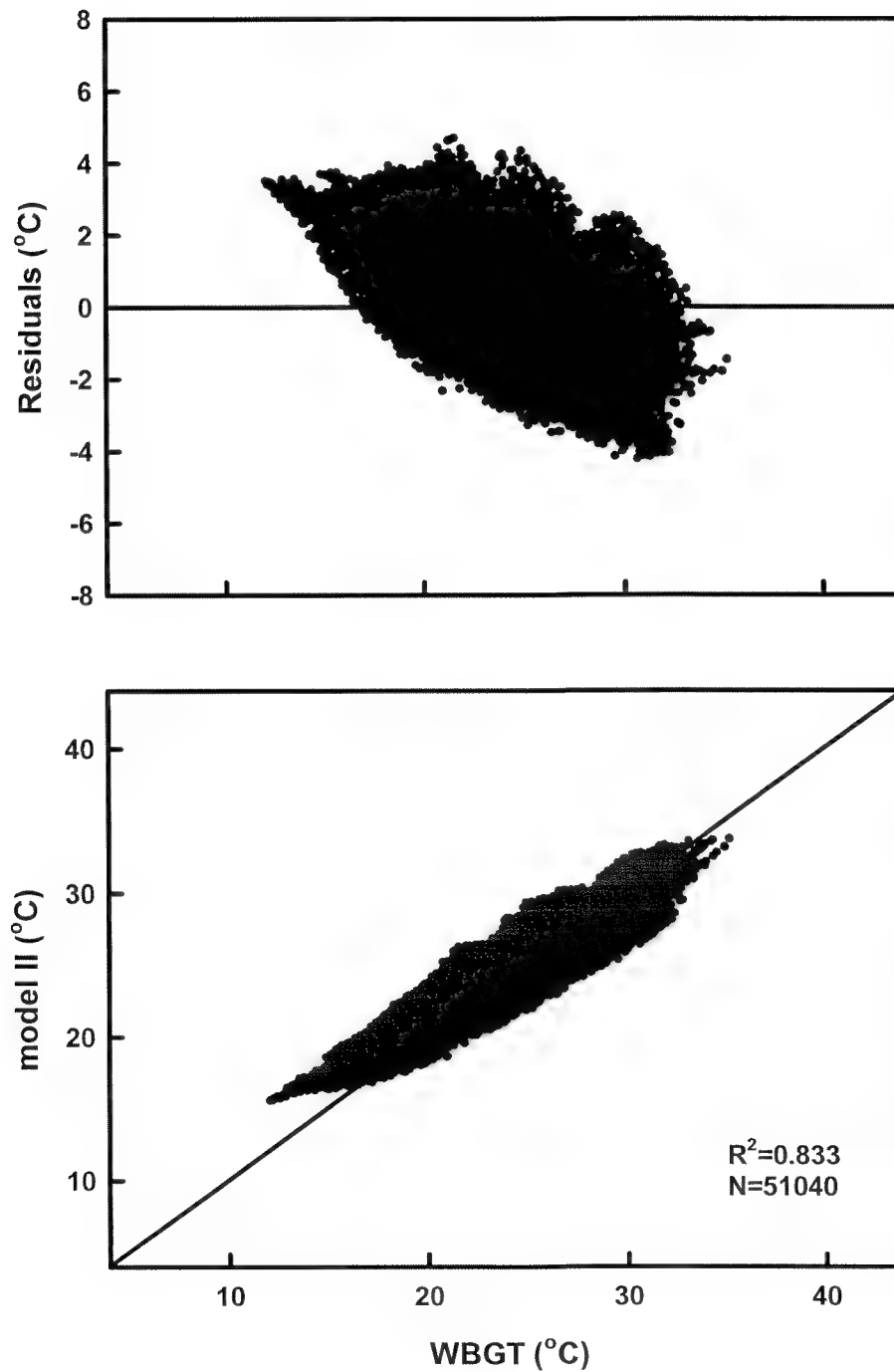
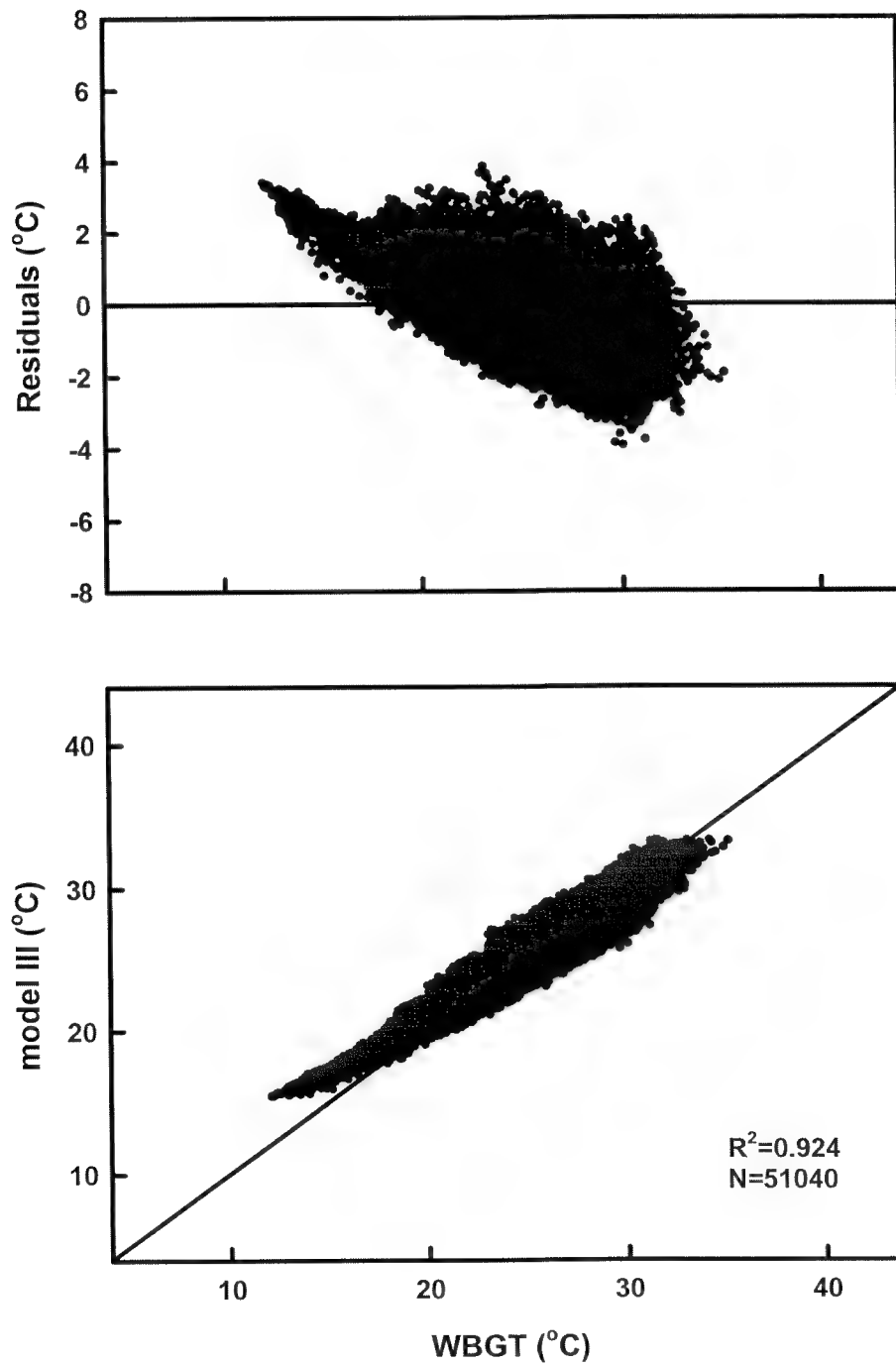


Figure 3. Comparison of a newly developed model (III) based on Ta, RH and solar radiation (SR), with the WBGT index showing correlation (bottom) and residuals scattergram (top). Database for this figure was collected from three stations in Israel.



Generally, in warm climates, when skin temperature (T_{sk}) is higher than T_a , air movement reduces heat load. Therefore, assuming that the wind velocity (V_a) component decreases the heat stress assessment in the environmental load (when $T_{sk} > T_a$), we subtracted the V_a from the WBGT predicted mode, as follows:

$$WBGT = 0.67357T_a + 0.07773RH + 0.00349SL - 0.10375V_a \text{ } ^\circ\text{C}; \quad .IV$$

Unfortunately, no significant improvement was found in the correlation coefficient (Figure 4) between this new prediction model (IV) and calculated WBGT ($R^2=0.925$), when compared to the correlation found for Model III ($R^2=0.924$), where V_a was not included in the WBGT prediction model.

UV Radiation

The UV measurements collected in Israel ranged from 0-31.51 $\text{W}\cdot\text{m}^{-2}$, whereas the simultaneous measurements of SR ranged from 0-1161 $\text{W}\cdot\text{m}^{-2}$. In spite of the low values of the UV measurements in relation to SR values, the UV variable was found to be significant in predicted WBGT. However, adding the UV component to the environmental stress prediction model did not improve the heat stress assessment. In fact, statistical analysis and a construction program for models development revealed that the UV component should be considered a minus term, and subtracted in the models that predict WBGT. This analysis contradicted our initial hypothesis, but might be explained by the fact that the SR measurements are already included the UV spectrum. Therefore, mathematically, not only do we not include the UV in predicted WBGT, we must also exclude it from the prediction model as it is already part of the measured SR. Thus, the newly constructed developed model, including UV radiation, was as follows:

$$WBGT = 0.66399T_a + 0.07857RH + 0.00836SR - 0.08574V_a - 0.18724UV \text{ } ^\circ\text{C}; \quad .V$$

This model (V) revealed a slightly improved correlation coefficient ($R^2=0.928$) with calculated WBGT (Figure 5) in comparison to the R^2 of Model IV. However, residual scattergrams ranged between -3° and 5°C values. Optimization of the constant for this model and applying it on $UV > 0.4 \text{ W}\cdot\text{m}^{-2}$ measurements revealed an improved index, as follows:

$$WBGT = 0.67706T_a + 0.09454RH + 0.0051SR - 0.10329UV - 0.14711V_a \text{ } ^\circ\text{C}; \quad .VI$$

This model (VI) revealed a higher correlation with WBGT of $R^2=0.933$ (Figure 6) and residual scattergram varying between -2° to 4°C . The last attempt of the model construction was to replace simultaneous SR measurements with UV measurements, as follows:

$$\text{WBGT}=0.68544T_a+0.07621\text{RH}+0.11812\text{UV}-0.11083V_a\text{ }^\circ\text{C}; \quad .\text{VII}$$

In general, according to the analysis of Model VII and the correlation coefficient ($R^2=0.909$) with calculated WBGT, UV can be considered a replacement for SR (Figure 7). However, depicted in Figure 13, this model (VII) overpredicted WBGT in the low environmental stress values and underpredicted the WBGT in the higher environmental stress values. In addition, the residual range increased, in comparison to Model V, from -4° to $+4^\circ\text{C}$.

Figure 4. Comparison of a newly developed model (IV) based on T_a , RH, SR and wind velocity (V_a), with the WBGT index showing correlation (bottom) and residuals scattergram (top). Database for this figure was collected from three stations in Israel.

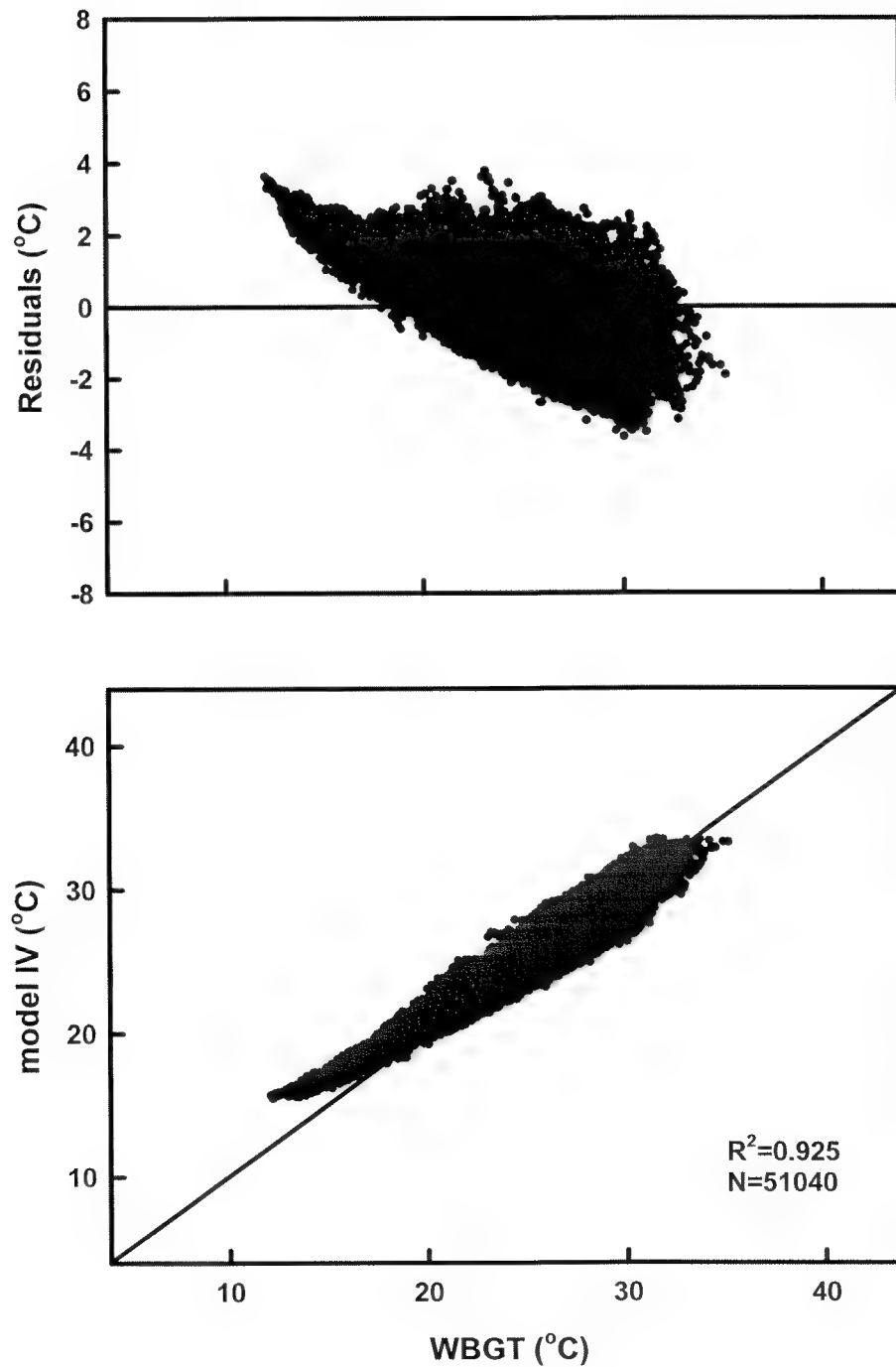


Figure 5. Comparison of a newly developed model (V) based on T_a , RH, SR, V_a and UV radiation with the WBGT index showing correlation (bottom) and residuals scattergram (top). Database for this figure was collected from three stations in Israel.

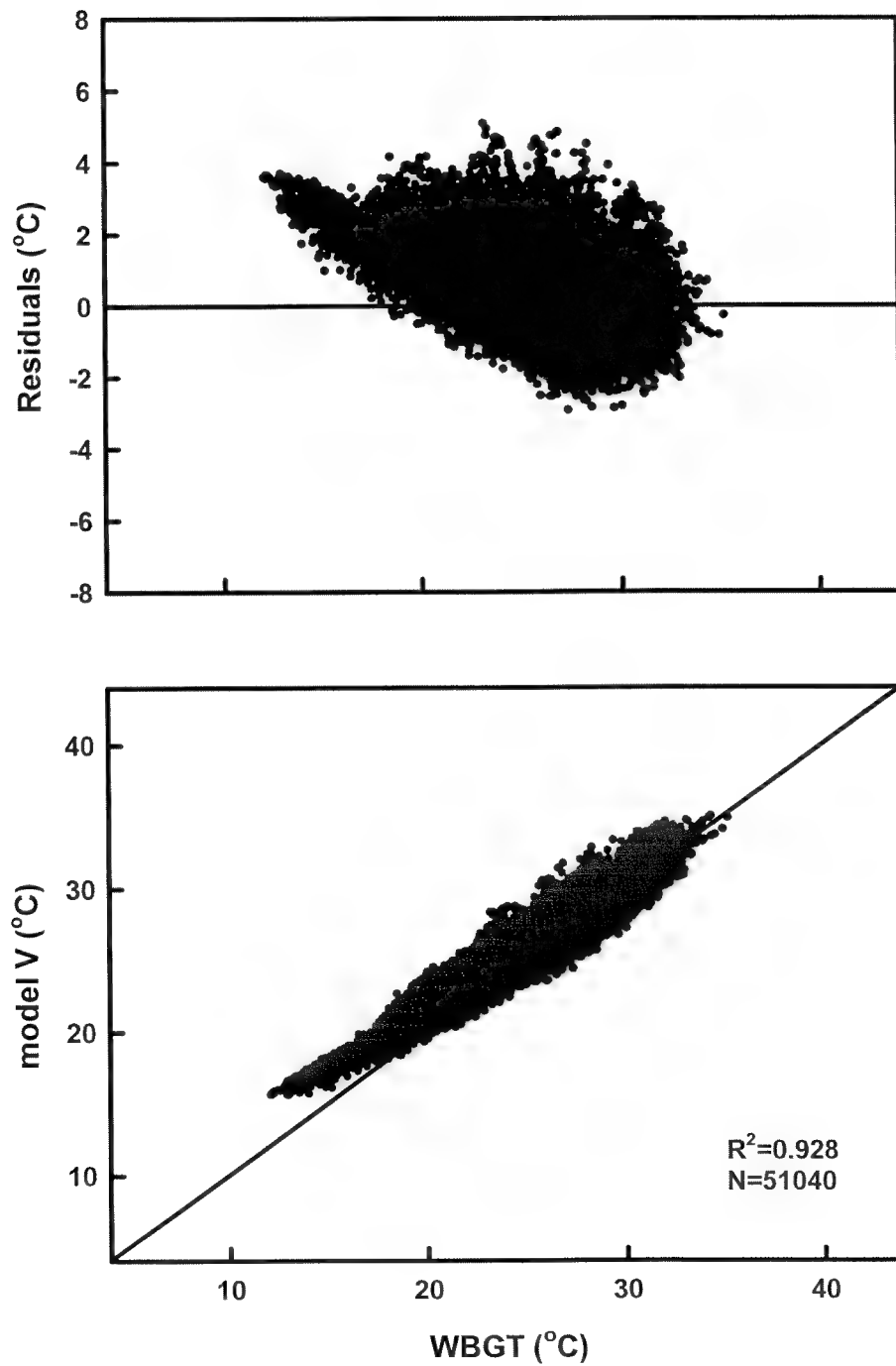


Figure 6. Comparison of a newly developed model (VI) based on T_a , RH, SR, V_a and $UV > 0.4 \text{ W}\cdot\text{m}^{-2}$, with the WBGT index showing correlation (bottom) and residuals scattergram (top). Database for this figure was collected from three stations in Israel.

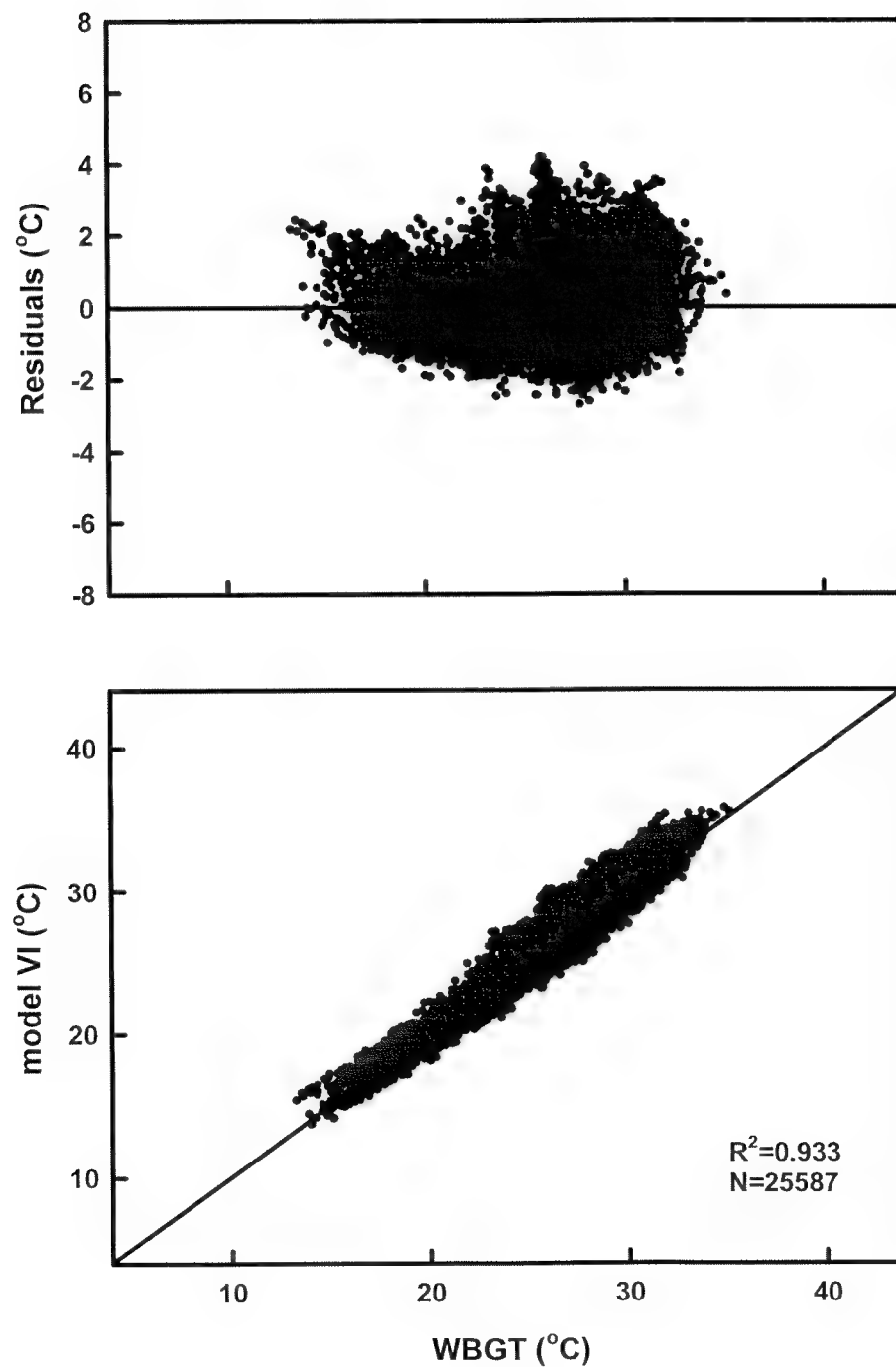
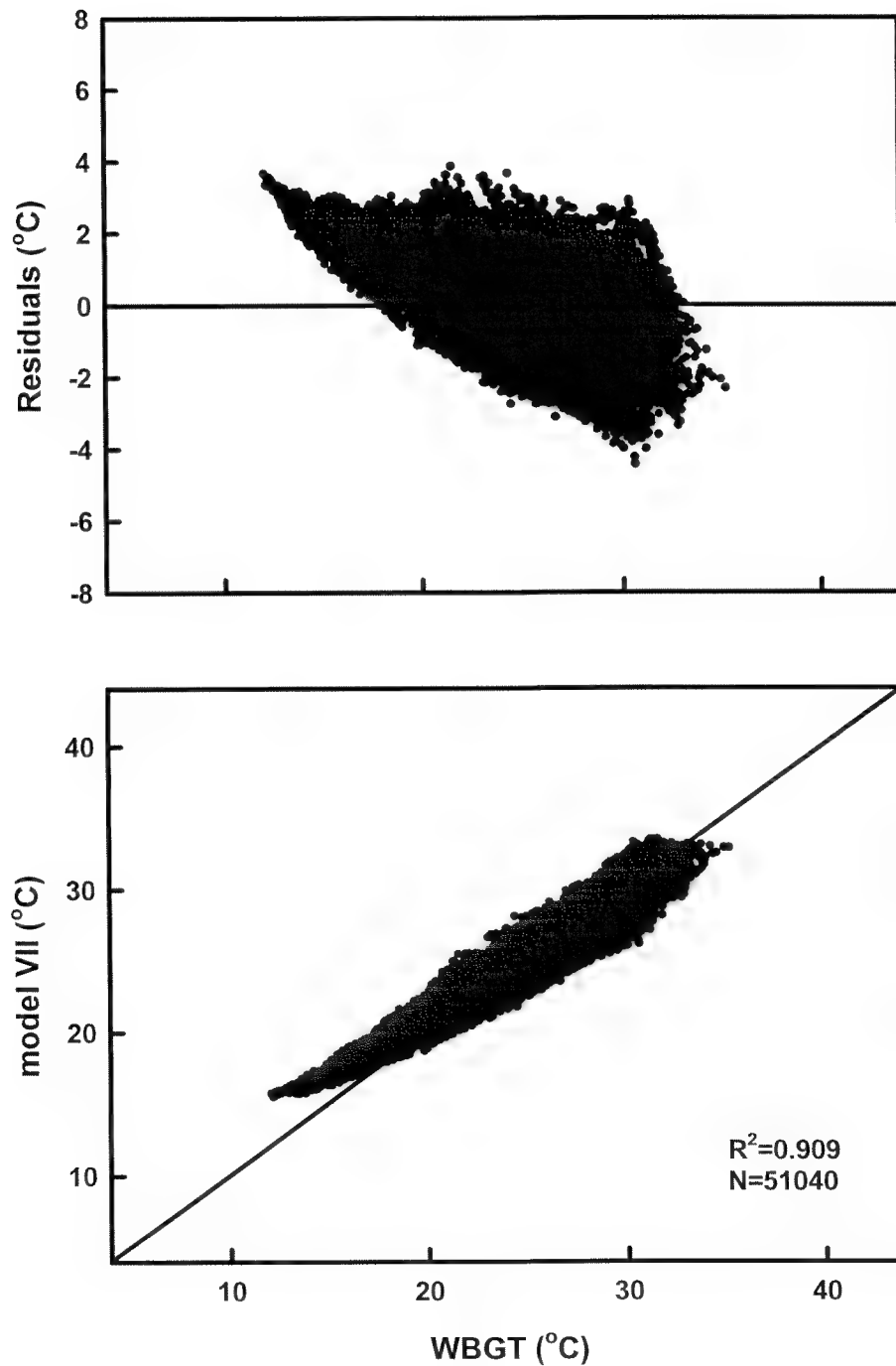


Figure 7. Comparison of a newly developed model (VII) based on T_a , RH, V_a and UV, with the WBGT index showing correlation (bottom) and residuals scattergram (top). Database for this figure was collected from three stations in Israel.



STUDY II – NEW ZEALAND

The data were collected over 60 days in February-March from 2 different locations on the south island: Kyle, which is near Christchurch, and Lauder, which is located between Dunedin and the west coast. In general, climatic conditions were more moderate than measured in the summer in Israel. There were over 18,000 measurements in a wide range for each variable as depicted in Table 2 (mean \pm SD).

Table 2. Mean (\pm SD) and range of environmental measurements collected in New Zealand. Data were collected from two different locations every 10 min over 24 hours for 60 days during February-March.

	T_a ($^{\circ}\text{C}$)	T_w ($^{\circ}\text{C}$)	RH (%)	T_g ($^{\circ}\text{C}$)	SR ($\text{W}\cdot\text{m}^{-2}$)	UV ($\text{W}\cdot\text{m}^{-2}$)	V_a ($\text{m}\cdot\text{sec}^{-1}$)
Mean \pm SD	14.83 \pm 5.02	11.15 \pm 3.05	65 \pm 21	18.86 \pm 9.48	228 \pm 307	13.80 \pm 18.01	3.36 \pm 2.40
Range	1.20-30.10	0.80-18.40	15-99	0.30-46.20	0-1161	0-68.60	0-16.20

The New Zealand database was used to evaluate and validate the newly developed Models I-VI, which were developed from the Israeli database. Applying Models I-IV for the New Zealand database revealed high correlation as depicted in Figure 8 for Model I, constructed from T_a ($R^2=0.882$); Figure 9 for Model II, constructed from T_a and RH ($R^2=0.915$); Figure 10 for Model III, constructed from T_a , RH and SR ($R^2=0.960$); and Figure 11 for Model IV, constructed from T_a , RH, SR and V_a ($R^2=0.955$). In fact, the correlation coefficients from the New Zealand database applied to these four models were higher than for the Israeli databases (Table 3). The residuals for New Zealand measurements were in a larger range than for Israel for Models II-IV, with overestimated values in low stress. However, these models were developed from the Israeli warmer climate conditions and purposed for heat stress assessments. Therefore, the overprediction residuals (Figs 9-11), which are in the low WBGT values ($<10^{\circ}\text{C}$), can be explained by measured T_a values $<15^{\circ}\text{C}$ that are not relevant to heat load evaluation.

Table 3. The correlation coefficient (R^2) between the WBGT index and the different predicted models, developed from the Israeli database and validated for the New Zealand database.

	Variables	The R^2 between WBGT and the newly developed models	
		Israel	New Zealand
Model No. I	T_a	0.687	0.882
Model No. II	T_a , RH	0.833	0.915
Model No. III	T_a , RH, SR	0.924	0.960
Model No. IV	T_a , RH, SR, V_a	0.925	0.955

Applying Model VI, which includes UV radiation, on the New Zealand database revealed with lower correlation ($R^2=0.686$) and spread residuals at wide variances of $\pm 8^\circ\text{C}$ (Figure 12). The latter results create cause for concern regarding the UV measurements and units from Israel and New Zealand, as the inverse impact of UV for New Zealand data was unexpected.

Figure 8. Validation of the newly developed model (I) based on T_a , with the WBGT index showing correlation (bottom) and residuals scattergram (top). Database for this figure was collected from two stations in New Zealand.

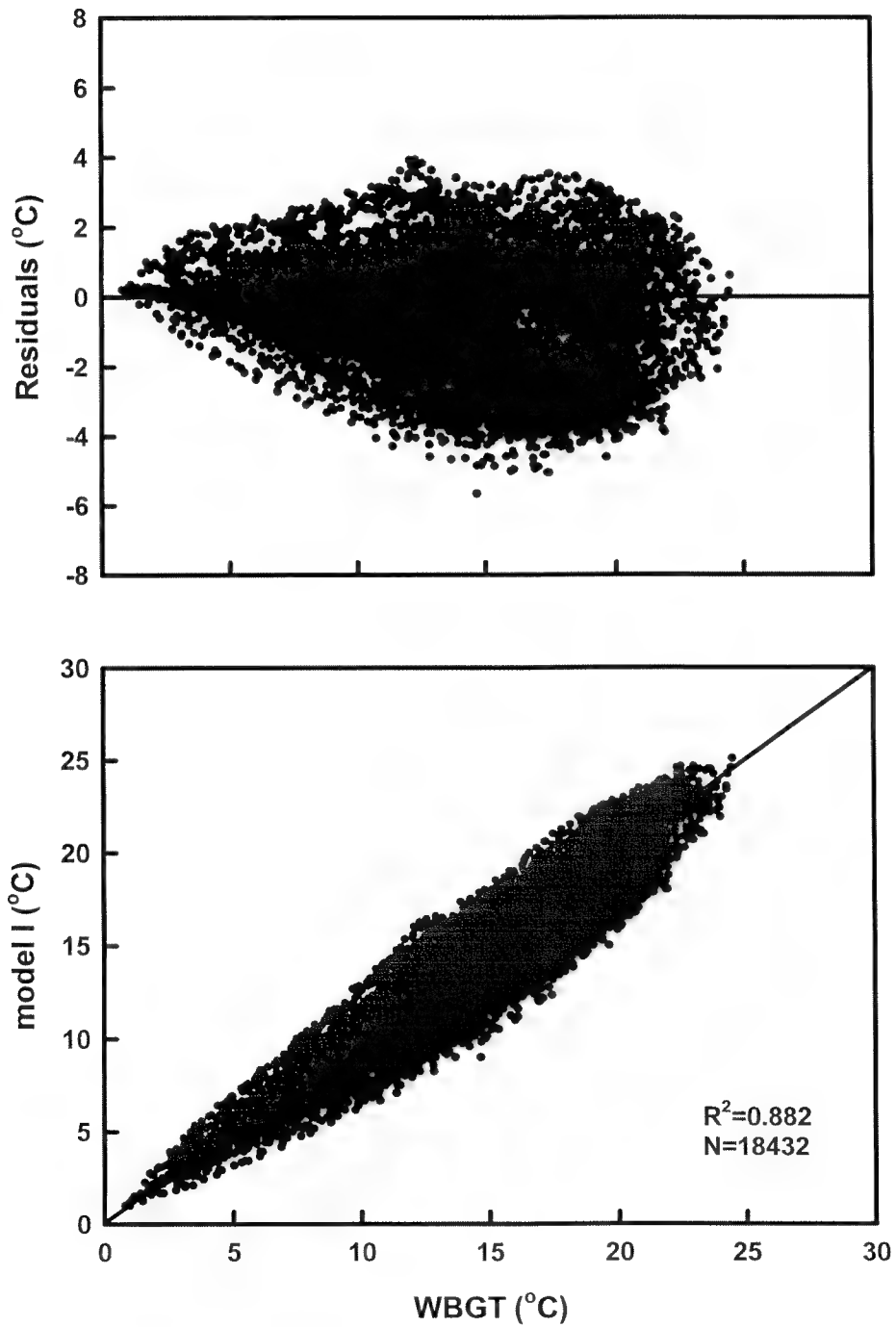


Figure 9. Validation of the newly developed model (II) based on T_a and RH, with the WBGT index showing correlation (bottom) and residuals scattergram (top). Database for this figure was collected from two stations in New Zealand.

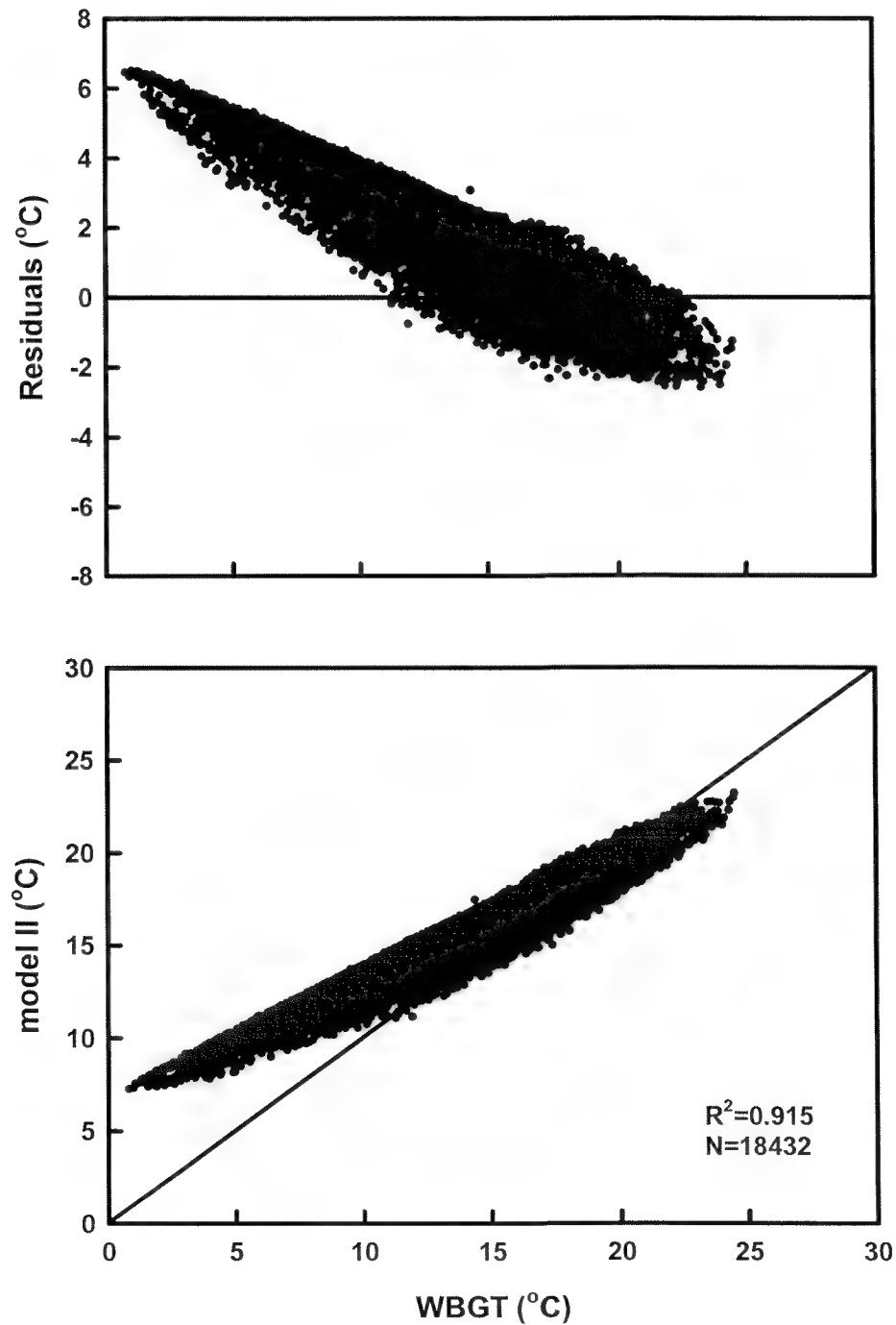


Figure 10. Validation of the newly developed model (III) based on T_a , RH and SR, with the WBGT index showing correlation (bottom) and residuals scattergram (top). Database for this figure was collected from two stations in New Zealand.

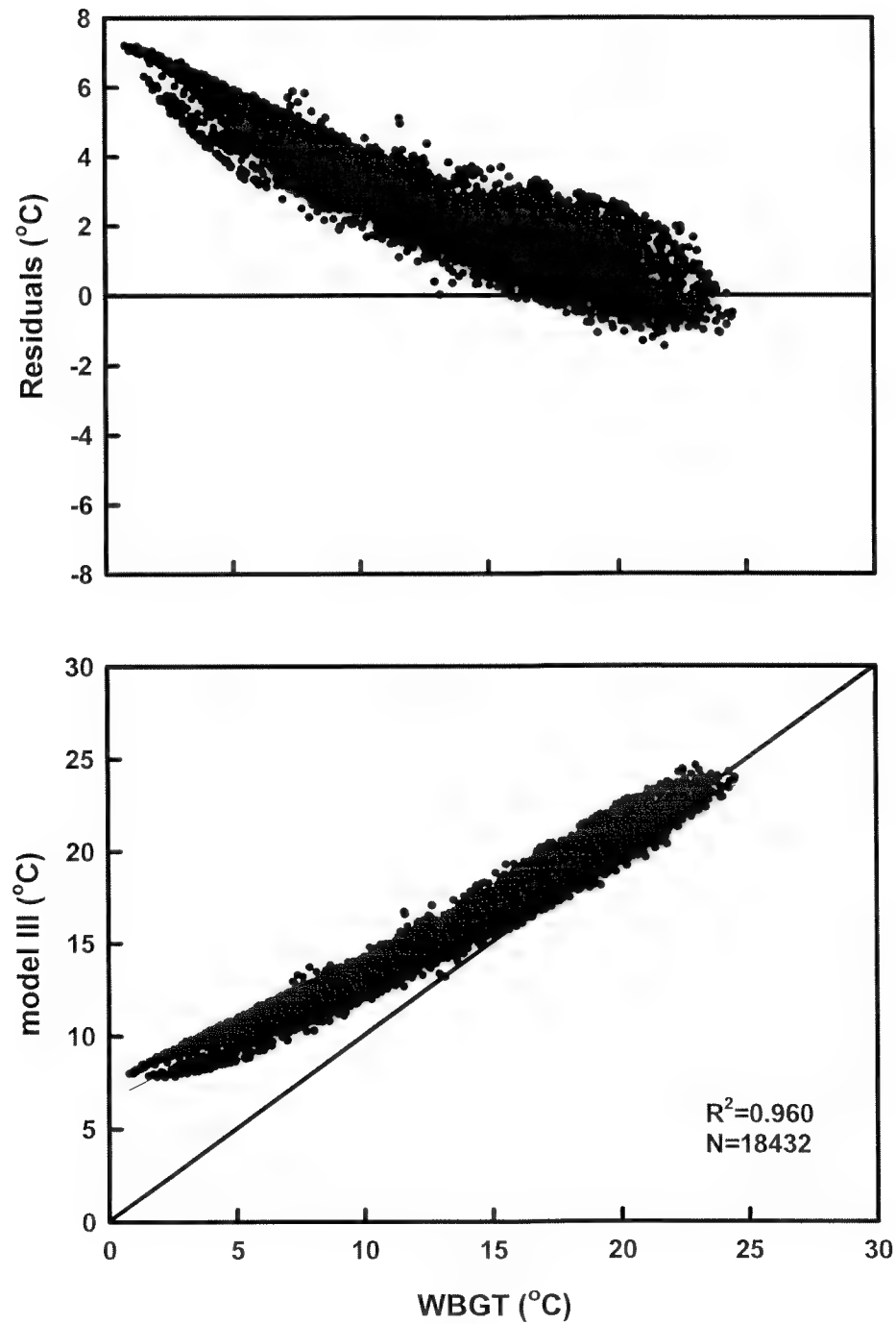


Figure 11. Validation of the newly developed model (IV) based on T_a , RH, SR and V_a , with the WBGT index showing correlation (bottom) and residuals scattergram (top). Database for this figure was collected from two stations in New Zealand.

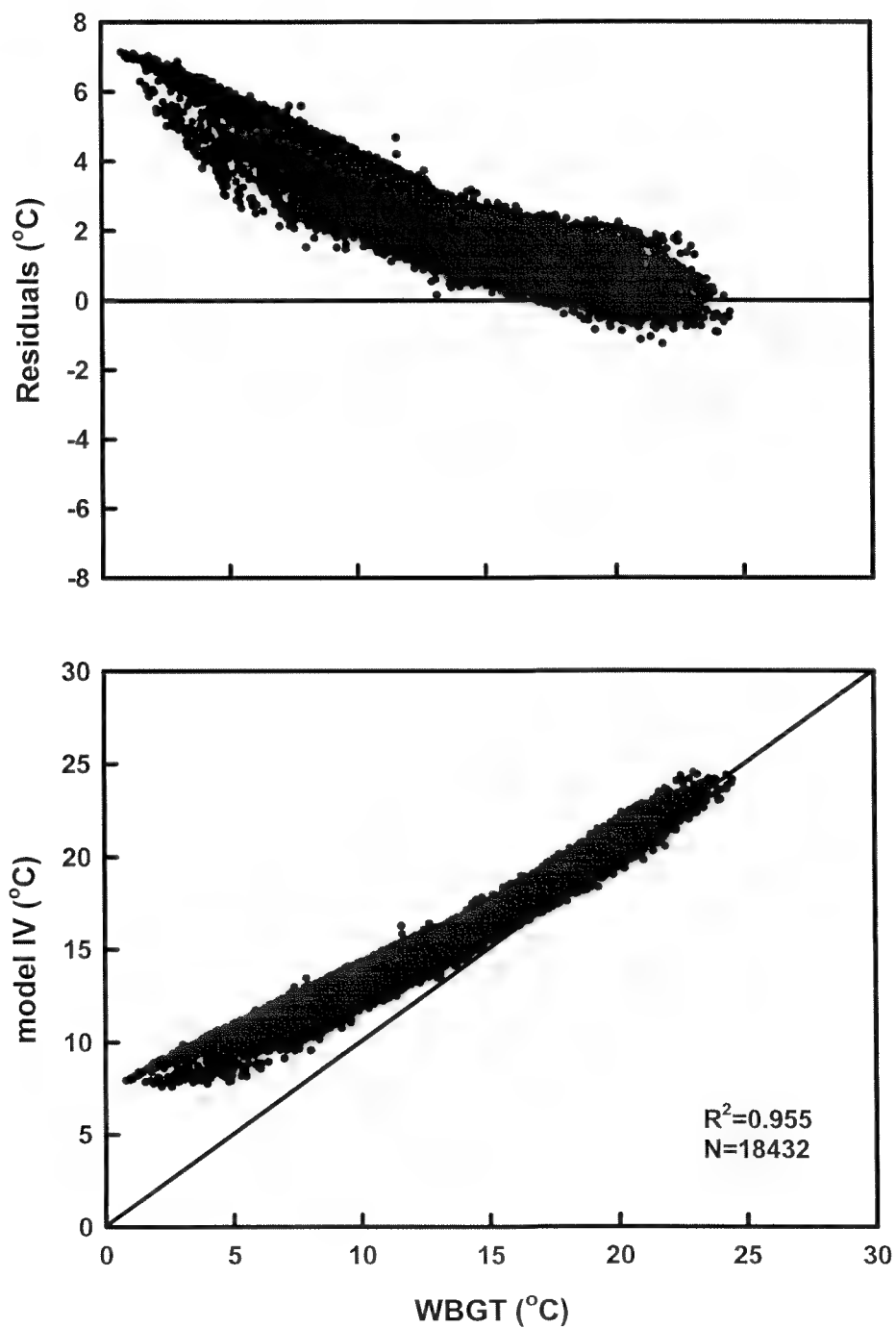
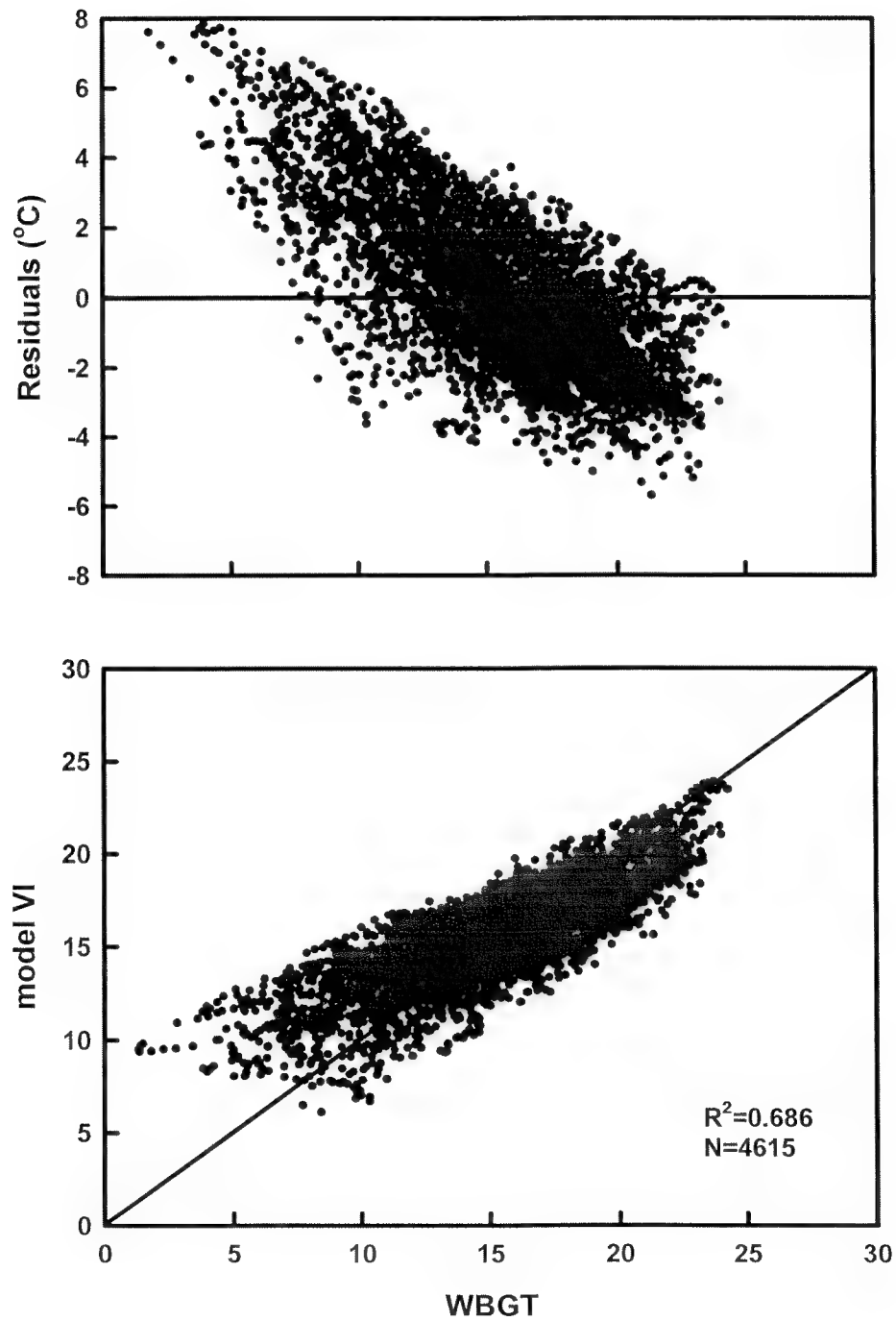


Figure 12. Validation of the newly developed model (VI) based on T_a , RH, SR, V_a and $UV > 0.4 \text{ W} \cdot \text{m}^{-2}$, with the WBGT index showing correlation (bottom) and residuals scattergram (top). Database for this figure was collected from one station in New Zealand.



VALIDATION OF ESI

Applying the ESI (15) to the Israeli databases from the three locations (Sdom, Jerusalem and Tel Aviv area) revealed high correlation ($R^2=0.959$) with the WBGT, and with residuals distributed symmetrically around the zero line as depicted in Figure 13. Applying ESI to the New Zealand databases from the two locations (Christchurch and Lauder) revealed an even higher correlation coefficient ($R^2=0.973$) between the ESI and the WBGT. However, the residuals were not distributed symmetrically around the zero line. Most of the residuals found under the zero line expressed underprediction of ESI for the WBGT (Figure 14). The explanation for the underpredicted values might be due to the difference in the GR spectrum. A relative comparison between the meteorological variables measured in Israel and New Zealand revealed that the main difference was in the UV radiation (Tables 1 & 2). Thus, at GR of $1100 \text{ W}\cdot\text{m}^{-2}$ in both New Zealand and Israel, we found that the UV values in New Zealand were twice as high as the values in Israel (e.g., 30 and $60 \text{ W}\cdot\text{m}^{-2}$). As a consequence, a correction factor might be needed for ESI to be used in the Southern Hemisphere where UV intensity is higher.

Figure 13. Comparison of the ESI with the WBGT index showing correlation (bottom) and residuals scattergram (top). Database for this figure was collected from three stations in Israel.

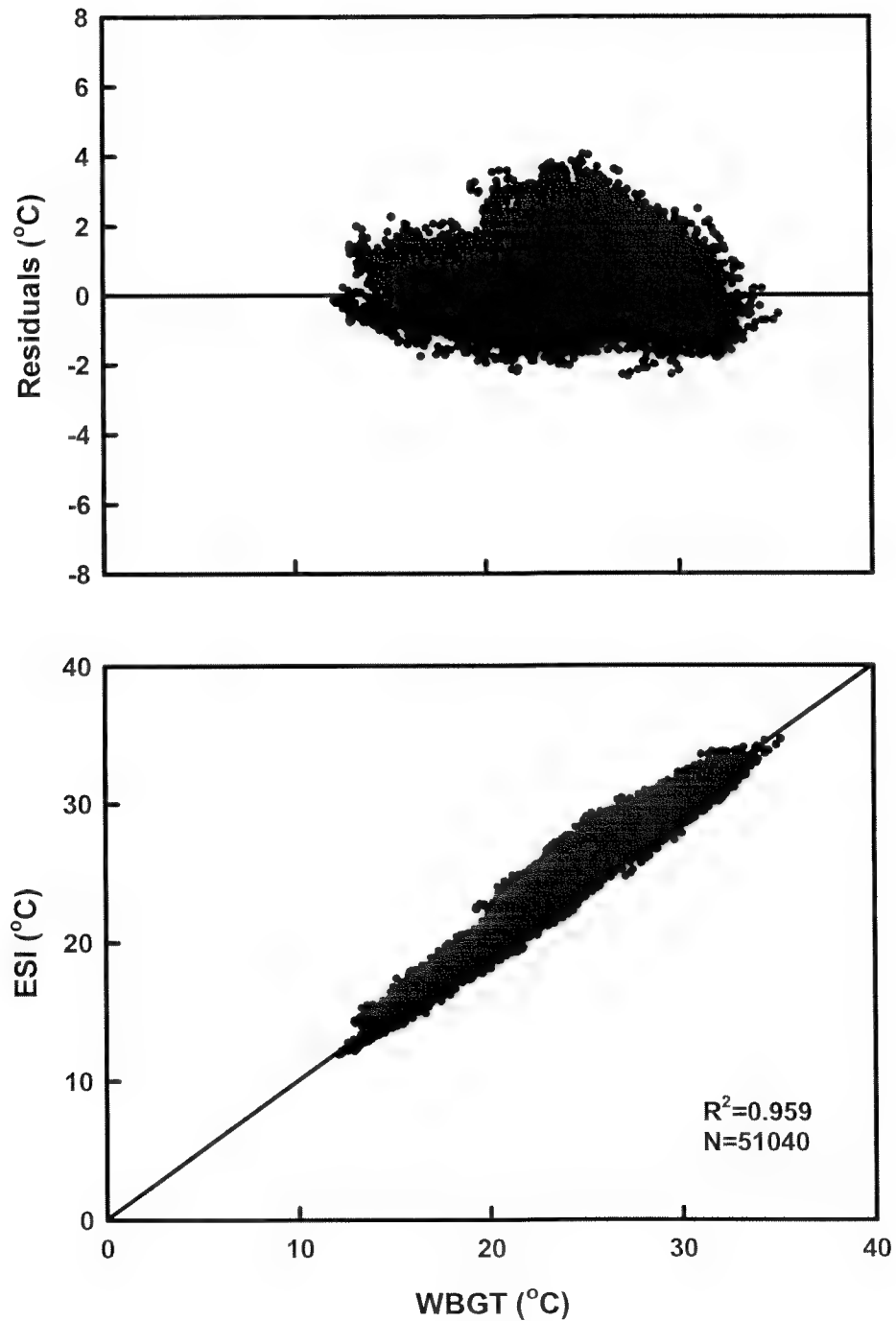
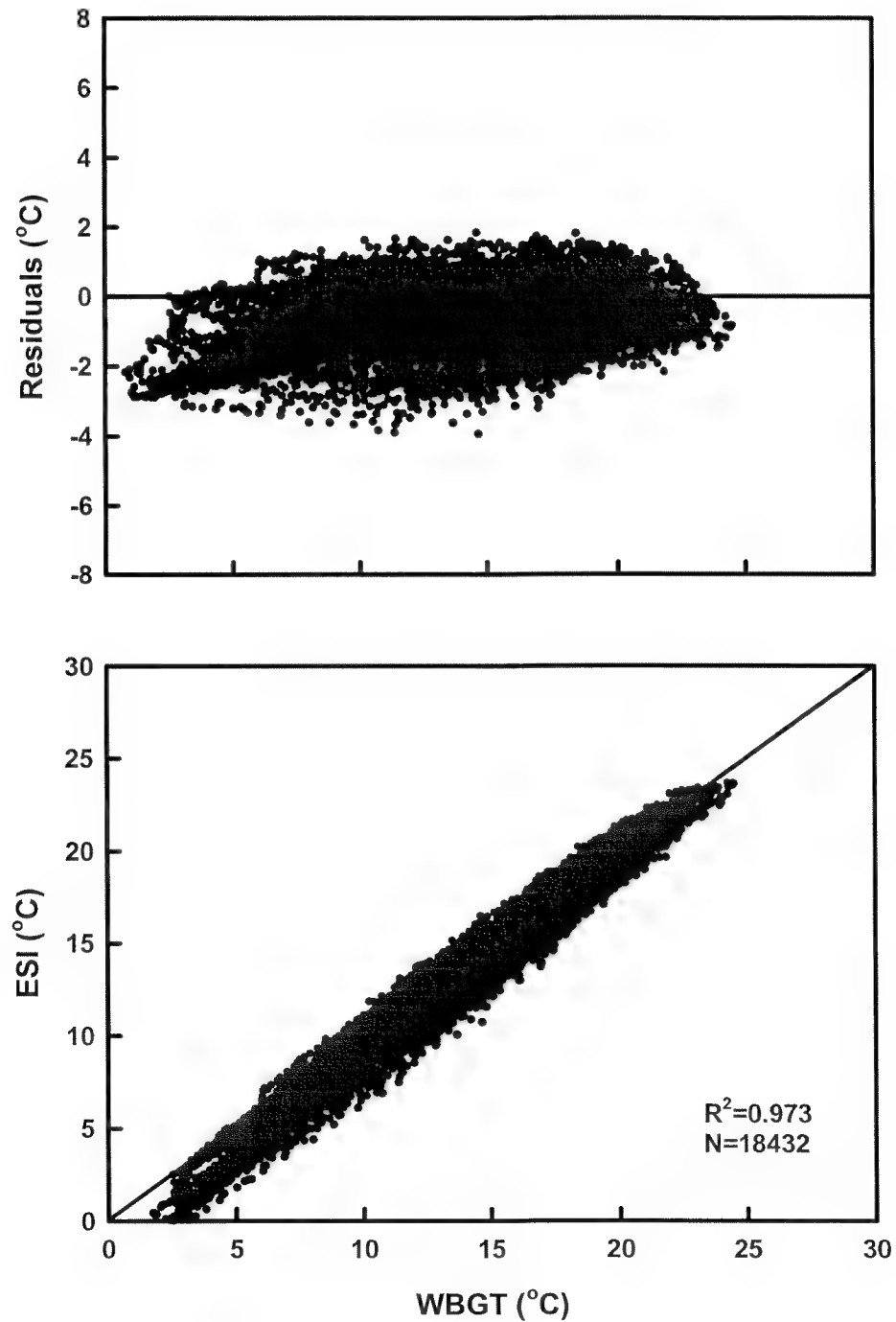


Figure 14. Comparison of the ESI, with the WBGT index showing correlation (bottom) and residuals scattergram (top). Database for this figure was collected from two stations in New Zealand.



DISCUSSION

Solar radiation is dominated by visible and near infra-red wavelengths. Only a small portion of this energy is within the UV region (11). Furthermore, only a small fraction of the amount of UV radiation at the outer edge of the atmosphere is transmitted to the earth's surface. This transmitted UV radiation is nevertheless of great importance because of the problems of increased sunburn, skin cancer, and eye diseases. The photon energies in the spectral region are sufficient to damage DNA. This has led us to believe that UV radiation should be included in the environmental stress assessment. However, results from this study indicated the limitations of UV applicability in the environmental stress assessment.

Two meteorological databases, consisting of T_a , RH, T_g , T_w , GR, V_a and UV radiation, were collected from two sites in New Zealand, where melanoma skin cancer rates are among the highest in the world (3,11). Data was also collected from two sites in Israel, including a site at the Dead Sea, located at the lowest point on earth (-400 below sea level) and characterized by a relatively high aerosol content due to its very high salt concentration. Analysis of these databases included attempts to construct a new environmental stress index based on different meteorological variables including UV radiation. However, the relatively high correlation found for the new models did not guarantee that the predictive ability would be suitable and applicable. Furthermore, the UV radiation component in the stress assessment was not significant and found to be a minus term, probably because UV is a portion in GR which was already included the model.

The intensity of UVB radiation is approximately two times smaller in magnitude than that of UVA, which is smaller by a factor of about 20 than the GR intensities. These relative magnitudes reflect the importance of GR in comparison to the UV radiation for the environmental stress assessment.

UV radiation has become a major public and scientific concern throughout the world. Increased public awareness of the possible impacts of changing UV radiation levels indicates a need for a UV index, which would show the level of the UV radiation intensity expected and recommend the necessary protective measures. However, it would be more useful if we could predict UV radiation from GR, simply because GR is a more common measured and used variable than UV radiation (8).

In Model VI we used the UV variable in addition to T_a , RH and V_a . Although the GR spectrum is from 280-2800 nm and the UV spectrum is from 280-400 nm, the UV component successfully replaced the GR component with a high correlation of $R^2=0.909$ when correlated between this Model (VI) and WBGT. According to these encouraging results, further studies should be executed in an attempt to predict UV radiation from GR.

ESI was developed and validated from large and different databases collected in Israel a few years ago (1). Applying this index to the current Israeli databases from the three different sites revealed high correlation ($R^2=0.959$) with WBGT, validating this index for environmental stress assessment. Furthermore, the higher correlation ($R^2=0.973$) found when applying the ESI to the databases from the two New Zealand sites strengthens the ESI for universal and world wide usage. However, the fact that ESI underestimated WBGT, in spite of the high correlation found, showed that it is probably due to the different GR component between the two countries. Therefore, further evaluation is necessary for establishing a correction factor for the southern hemisphere.

Ultraviolet highly correlated with ambient temperature in Israel. However, in New Zealand, where measured T_a was lower than in Israel ($14.83\pm5.02^\circ\text{C}$ and $28.23\pm5.82^\circ\text{C}$, respectively), UV was not necessarily correlated with T_a and was dependent more on open sky conditions. Thus, although we recognize the importance of UV as a meteorological variable, we can find the same high value (e.g., $40 \text{ W}\cdot\text{m}^{-2}$) in ambient temperature of 15°C and in 40°C . As a consequence, we concluded that the ESI should include GR rather than UV, and because of health hazards, an independent UV index should be implemented and used separately whenever there is an open sky. This does not necessarily have to take place in the summer.

In summary, the ESI should include GR rather than UV radiation. However, because of the health hazards of UV radiation, an independent index parallel to the ESI should be considered and used for safety measures and as guidelines for protection from UV radiation. The UV index has greater potential for acceptance by laymen if GR is incorporated in its derivation, which is a more commonly measured and used variable than UV radiation. The latter can be done practically by further studying the inter relationships between GR and UV radiation.

CONCLUSIONS

Prolonged sun exposure results in damage to the skin, sub-cutaneous structures, and the immune system from UV radiation. The long-term clinical presentation of this damage includes the appearance of skin nevi, premature

aging of the skin, cataract formation, increased infectious and inflammatory diseases, and an increased incidence of various types of skin cancer. However, there is no place for the UV radiation variable in the environmental stress assessment because of the inclusion of GR in ESI.

An independent UV index should help in preventing acute and chronic injury from this unseen threat. Thus, a prediction of UV radiation from GR would be a great benefit of such an index. Furthermore, the numerical grading of the magnitude of UV radiation will enable the implementation of practical guidelines pertaining to work-rest cycles, and safety measures, such as clothing and other protective devices. In final conclusion, a new device for GR measurement, which enables the user easy calculation of UV radiation by a new algorithm, might be a useful and essential tool for the US Armed Forces.

REFERENCES

1. Afak, F., and H. Mukhtar. Effects of solar radiation on cutaneous detoxification pathways. *J. Photochem. Photobiol.* 63: 61-9, 2001.
2. Armstrong, B., and K. A. Kricker. The epidemiology of UV induced skin cancer. *J. Photochem. Photobiol.* 63: 8-18, 2001.
3. Cox, B., and B. Coombs. Trends in Melanoma of the skin in New Zealand. *Transactions of Menzies Foundations.* Vol 15, 1989.
4. Decraene, D., P. Agostinis, A. Pupe, P. de Haes, and M. Garmyn. Acute response of human skin to solar radiation: regulation and function of the p53 protein. *J. Photochem. Photobiol.* 63: 78-83, 2001.
5. Gibson, J. H.. UVB Radiation – definition and characteristics. http://uvb.nrel.colostate.edu/publications/uvb_primer.pdf.
6. Hightower, K. R. A review of the evidence that ultraviolet irradiation is a risk factor for cataractogenesis. *Doc. Ophthalmos.* 88: 205-220, 1994.
7. Information Sheet on Solar Radiation. National Institute of Water & Atmospheric Research of New Zealand (NIWA) www.katipo.niwa.cri.nz.
8. Kudish, A. I., and E. Evseev, Statistical relationship between solar UVB and UVA radiation and global radiation measurements at two sites in Israel. *Int. J. Climatol.* 20: 759-770, 2000.
9. Malina, L. Effects of ultraviolet radiation on the immune system and the effect of exogenous photoprotective agents on the ultraviolet radiation induced immunosuppression. *Cas. Lek. Cesk.* 141: 338-342, 2002.
10. McKenzie, R. L. Application of a simple model to calculate latitudinal and atmospheric differences in ultraviolet radiation. *Weather and Climate.* 3-114, 1991.
11. McKenzie, R, D. Smale, and G. Bodeker. Ozone profile differences between Europe and New Zealand: Effect on surface UV irradiance and its estimation from satellite sensors. *J. Geophysical Research* 108: 1-9, 2003.
12. Miller, A. J., C. Long, H. Lee, and J. D. Wild. Experimental ultraviolet index, presented at WMO Experts meeting on UVB. Les Diablerets, Switzerland, July, 1994.
13. Moehrle, M., M. Soballa, and M. Korn. UV exposure in cars. *Photodermatol Photoimmunol Photomed.* 19(4): 175-181, 2003.

14. Moran, D., K. B. Pandolf, Y. Shapiro, Y. Heled, Y. Shani, W. T. Matthew, and R. R. Gonzalez. An environmental stress index (ESI) as a substitute for the wet bulb globe temperature (WBGT). *J. Therm. Bio.* 26: 427-31, 2001.
15. Moran, D. S., K. B. Pandolf, A. Laor, Y. Heled, W. T. Matthew, and R. R. Gonzalez. Evaluation and refinement of the environmental stress index for different climatic conditions. *J Basic Clin Physiol Pharmacol.* 14: 1-15, 2003.
16. O'Brien, J. P., and W. Regan. A study of elastic tissue and actinic radiation in "aging", temporal arteritis, polymyalgia rheumatica, and atherosclerosis. The actinic storm in the modern world. *J. Am. Acad. Dermatol.* 24: 765-776, 1991.
17. Ralston, M. L., and R. L. Jennrich. DUD – a derivative free algorithm for non-linear least squares. *Technometric.* 20: 7-14, 1978.
18. Rosso, S., R. Zanetti, C. Martinez, M. J. Tormo, S. Schraub, H. Sancho-Garnier, S. Franceschi, L. Gafa, E. Perea, C. Navarro, R. Laurent, C. Schrameck, R. Talamini, R. Tumino, and J. Wechsler. The multicentre south European study 'Helios'. II: Different sun exposure patterns in the aetiology of basal cell and squamous cell carcinomas of the skin. *Br. J. Cancer.* 73: 1447-1454, 1996.
19. Seckmeyer, S., and R. L. McKenzie. Increased ultraviolet radiation in New Zealand (45S) relative to Germany (48N). *Nature* 359: 135-137, 1992.
20. Termorshuizen, F., R. B. Geskus, M. T. Roos, R. A. Countinho, H. Van Loveren. Seasonal influences on immunological parameters in HIV-infected homosexual men: searching for the immunomodulating effects of sunlight. *Int. J. Hyg. Environ. Health.* 205:379-384, 2002.
21. Werth, V. P., K. J. Williams, E. A. Fisher, M. Bashir, J. Rosenbloom, and X. Shi. UVB irradiation alters cellular responses to cytokines: role in extracellular matrix gene expression. *J. Invest. Dermatol.* 108: 290-294, 1997.
22. Whiteman, D. C., C. A. Whiteman, and A. C. Green. Childhood sun exposure as a risk factor for melanoma: a systematic review of epidemiologic studies. *Cancer Causes Control.* 12: 69-82, 2001.
23. WMO. Scientific assessment of ozone depletion: *WMO Global Ozone Research and Monitoring Report No. 37*, Geneva, 1994.
24. Yaglou, C. P., and D. Minard. Control of heat casualties at military training centers. *Arch. Ind. Hlth.* 16: 302-305, 1957.

APPENDIX A. Mean (\pm SD) and range of the environmental measurements at the different stations in Israel and New Zealand. Data were collected for 4 months in Israel during June-September and for 2 months in New Zealand during February-March.

Israel

Station	T_a (°C)	T_w (°C)	RH (%)	T_g (°C)	SR (W·m ⁻²)	UV (W·m ⁻²)	V_a (m·sec ⁻¹)
Jerusalem	24.12 \pm 4.53	17.89 \pm 2.16	59 \pm 23	28.46 \pm 9.65	313 \pm 374	7.99 \pm 9.77	4.03 \pm 1.80
N=17452	13.90-40.60	9.92-23.64	8-99	10.80-56.10	0-1171	0.0-30.0	0.0-11.10
Bet-dagan	26.72 \pm 3.73	22.46 \pm 2.22	69 \pm 15	32.66 \pm 8.27	294 \pm 355	6.56 \pm 9.41	3.15 \pm 1.65
N=17204	15.60-43.40	13.80-27.90	11-102	15.30-58.20	0-1089	0.0-31.51	0.0-9.70
Sdom	34.20 \pm 3.62	21.75 \pm 2.35	35 \pm 11	37.71 \pm 9.44	293 \pm 356	6.34 \pm 9.22	3.91 \pm 2.14
N=16384	24.10-45.40	11.63-27.14	13-69	19.90-60.00	0-1045	0.0-30.30	0.0-12.60

New Zealand

Station	T_a (°C)	T_w (°C)	RH (%)	T_g (°C)	SR (W·m ⁻²)	UV (W·m ⁻²)	V_a (m·sec ⁻¹)
Lauder	15.01 \pm 6.11	10.53 \pm 3.44	59 \pm 23	18.81 \pm 10.64	225-299	13.80 \pm 18.01	3.69 \pm 3.01
N=8360	1.20-28.80	0.80-18.10	15-99	0.30-45.80	0-1161	0-68.60	0-16.20
Christchurch	14.66 \pm 3.76	11.72 \pm 2.50	71 \pm 18	18.91 \pm 8.30	231 \pm 315		3.05 \pm 1.61
N=9216	4.10-30.10	2.40-18.40	15-97	1.70-46.20	0-1135		0-10.20